Title
Fuel Cell/Gas Turbine Hybrid System Control for Daily Load Profile and Ambient Condition Variation

Journal
Journal of Engineering for Gas Turbines and Power, 132(1)

ISSN
0742-4795

Authors
Roberts, Rory A
Brouwer, Jack
Samuelsen, G Scott

Publication Date
2010

DOI
10.1115/1.2833489

Fuel Cell/Gas Turbine Hybrid System Control for Daily Load Profile and Ambient Condition Variation

Rory A. Roberts

Jack Brouwer

G. Scott Samuelsen
e-mail: gss@uci.edu

National Fuel Cell Research Center,
University of California,
Irvine, CA 92697

Fuel Cell/Gas Turbine (FC/GT) hybrid technology is promising, but introduces challenges in system operation and control. For base-load applications, changes in ambient conditions perturb the system and it becomes difficult to maintain constant power production by the FC/GT system. If the FC/GT hybrid system is load-following, then the problem becomes even more complex. In the current study, a dynamic model of a FC/GT power plant is developed with system controls. Two cases are evaluated: (1) system controls are developed to maintain constant power and process control within acceptable constraints and (2) the FC/GT power plant is set in power following mode connected in parallel to the grid for a daily load profile scenario. Changing ambient conditions are employed in the dynamic analysis for both cases. With appropriate attention to design of the system itself and the control logic, the challenges for dynamic system operation and control can be addressed. [DOI: 10.1115/1.2833489]

Keywords: fuel cell, gas turbine, hybrid, controls, dynamic simulation, base-load

Introduction

Hybrid cycles comprised of high temperature fuel cells, such as molten carbonate fuel cells (MCFCs) or solid oxide fuel cells (SOFCs), will likely be the preferred method for generating electric power in the future, initially at the small to medium scale (250 kW to 20 MW), and later in large scale central plants (>100 MW). However, hybrid FC/GT systems are in need of significant advancement before they are introduced as commercial products. Some progress is needed to address the specific challenges that are introduced by coupling a fuel cell with a gas turbine given their disparate dynamic response characteristics.

Several entities around the world have developed steady state simulation capabilities for FC/GT systems. These include efforts of the Georgia Institute of Technology [1], the University of Genova [2–4], NFCRC [5–7], and others. Dynamic FC/GT simulation capabilities are less common, but are increasingly being developed as the demand for dynamic understanding and control development grows. Examples of previous dynamic simulation efforts include the work of University of Genova, National Energy Technology Laboratory (NETL) [7–9], FuelCell Energy [10–12], and the National Fuel Cell Research Center (NFCRC) [13–18].

Hybrid systems are sensitive to ambient conditions due the sensitivity of compressors to air density. At higher temperatures the air becomes less dense requiring a compressor to do more work to pressurize and move the air through the system. As for a hybrid system, it is challenging to maintain sufficient compressor mass flow for extreme conditions since the fuel cell is operated at a fixed temperature. If the gas turbine operates at a fixed speed, there are no options for controlling the mass flow. The total power output of the system may have to be sacrificed in order to maintain appropriate fuel cell operating temperature by lowering the load demand on the fuel cell.

Manuscript received June 16, 2006; final manuscript received September 21, 2007; published online October 1, 2009. Review conducted by Dilip R. Ballal. Paper presented at the ASME Turbo Expo 2006 Power for Land, Sea, & Air, Barcelona, Spain, May 8–11, 2006, Paper No. GT2006-90741.

Background

NFCRC has developed dynamic modeling tools for FC/GT hybrid systems. In previous work [16–18], transient performance and controls analyses of atmospheric hybrid systems with MCFCs were presented. Load perturbations were implemented to analyze the MCFC/GT hybrid response. In these investigations it was discovered that additional control loops are necessary to control the MCFC operating temperature. For example, varying fuel utilization across the MCFC provided some means for control but was limited. Variable speed operation of the gas turbine was tested and showed more promise, but still was limited in the particular system at lower power demands. For a larger turn-down in system power a bypass or auxiliary combustor is needed in parallel [14].

For part-load operation of a FC/GT hybrid, it has been shown that a variable speed gas turbine is a required feature for both pressurized [2] and atmospheric systems [15]. The variable speed gas turbine provides better control of the compressor mass flow.

In previous work, a system model was developed and compared to experimental data from the Siemens Power Corporation (SPC) SOFC/GT system [15]. A dual shaft turbine was used in SPC SOFC/GT system. The dual shaft turbine prevented the direct control of the compressor mass flow, which limited operational flexibility. The system had to be operated at the maximum power safely allowed.

In the current paper, a 1.15 MW pressurized SOFC/GT hybrid model is developed. A diagram of the system is presented in Fig. 1 and a schematic of the SOFC module is presented in Fig. 2. The system was designed around the Capstone C200 micro-turbine generator. Design parameters for the C200 [19] and the hybrid plant are presented in Table 1.

Dynamic Model. The components making up the dynamic model are the same as those presented in earlier work [14–17]. The electrochemical performance for the SOFC is based on the results presented by Kim et al. [20]. The following polarization equations are derived in terms of current density with units of current per area. This is to allow for a more straightforward comparison between fuel cells of various sizes. An anode supported planar SOFC is assumed in this study.

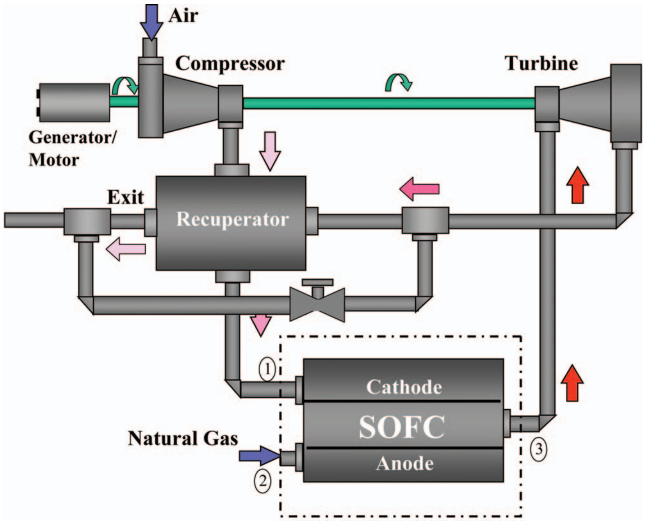

Fig. 1 Pressurized SOFC/GT hybrid cycle

In general, the most significant polarization (loss) inherent to high temperature fuel cells is cell resistance. At normal operating conditions, this is primarily due to low ionic and electronic conductivity of the high temperature materials associated with the electrolyte, anode and cathode, and interconnect conduction paths. Resistance can also be high if the cell is operating at a temperature below the optimum temperature due to the strong temperature dependence of electrolyte ionic resistivity. The loss in cell potential associated with resistance is given by Ohm's law:

$$\eta_R = iR_{\text{eff}} \tag{1}$$

Experimental data are available for measured values of resistances at various temperatures. The internal resistance is empirically fitted to the form of $\ln(R_{\text{eff}}/T)$ versus $1/T$.

Therefore,

$$\ln(R_{\text{eff}}/T) = 7509.6(1/T) - 25.855$$

$$R_{\text{eff}}(T) = T\exp(7509.6(1/T) - 25.855) \tag{2}$$

The electrochemistry provided by Kim et al. is for a single cell test. Therefore, for cell-to-stack performance, additional resistance is added to account for the resistance of interconnects, terminal blocks, and other electrical components of the stack. The amount of resistance between cells and stack connection was justified to be constant with temperature and added to achieve typical performances of SOFC stacks today [21].

Losses associated with sluggish kinetics due to low temperatures, poor availability of active electrocatalytic sites, triple-phase boundary kinetics, and/or solution and dissolution kinetics are

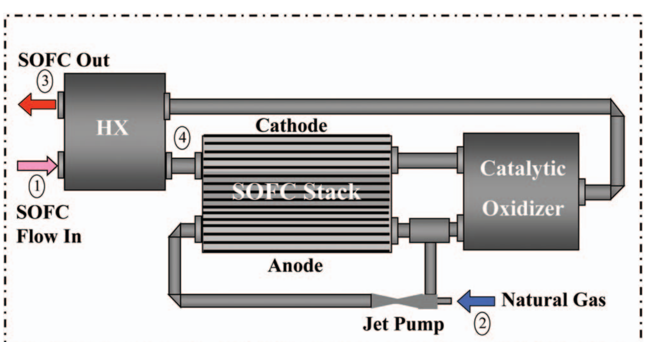

Fig. 2 SOFC module

Table 1 Design parameters for the SOFC/GT system

Design Parameter	Value	Unit
System		
System Power	1150	kW
Combustor Efficiency	1	
Recuperator Effectiveness	1	
Heat Exchanger Effectiveness	0.4	
System Efficiency	0.73	
Gas Turbine		
Shaft Speed[a]	60,000	RPM
Turbine Inlet Temperature[a]	950	C
Turbine Efficiency	90.0%	
Mass Flow[a]	1.3	kg/sec
Compressor Inlet Temperature	15	C
Compressor Discharge Pressure[a]	435.7	kPa
Compressor Efficiency	75.0%	
Gas Turbine Power Mechanical Loss (Shaft)	$(\text{RPM}^2)8.33\times10^{-10}$	kW
Gas Turbine Power Electronics Efficiency	98% and 14 kW load	
Compressor Leakage	0.02	
Compressor Filter Loss	0.02	
SOFC Module		
SOFC Stack Power	960	kW
SOFC Active Area	320	m^2
Current Density	4000	A/m^2
SOFC Operating Voltage	0.75	V
SOFC Power Electronics	100.0%	
Anode Recirculation	80.0%	
SOFC Stack Fuel Utilization	85.0%	
SOFC Average Operating Temperature	900	C

[a]Willis, 2005

modeled using a relationship for activation polarization. At reasonably high current densities typical of an operating cell, this polarization can be simulated by the simplified Tafel equation. The Tafel activation polarization equation can be reduced to Eq. (3). The Tafel equation is only valid for $i > i_0$. The operation range of the SOFC in this study is consistently above this limit. Therefore, applicability of the Tafel equation is an adequate assumption in this study:

$$\eta_A(i) = \frac{R_u T}{\alpha n F}\ln\left(\frac{i}{i_0}\right) \tag{3}$$

The transfer coefficient α is typically approximately 0.5 and accounts for the distribution of intermediate species at the triple-phase boundary, indicating whether these species more closely resemble reactants or products and may be quantified through experimental data. The exchange current density i_0 is dependent on temperature, pressure, and material properties. Assuming constant pressure operation Eqs. (4) and (5) provide i_0 and α, respectively, as a function of temperature [20]:

$$i_o = -0.37T^2 + 78.84T - 40{,}711 \tag{4}$$

$$\alpha = -5.73\times10^{-6}T^2 + 1.35\times10^{-2}T - 6.9 \tag{5}$$

Concentration polarization is associated with concentration gradients near the active cell surface and is dominated by the rate of diffusion of the gases through the porous electrodes as mentioned earlier. Equation (6) is the general equation used for modeling of the concentration loss in an anode supported fuel cell. The limiting current density is dependent on the partial pressures, temperatures, and the diffusivity of the electrode materials:

$$\eta_C(i) = \frac{R_u T}{2F} \ln\left(1 - \frac{i}{i_{L(a)}}\right) - \frac{R_u T}{2F} \ln\left(1 + \frac{P^0_{H_2} i}{P^0_{H_2O} i_{L(a)}}\right) \quad (6)$$

i_L is the limiting current density and is the most important parameter in Eq. (6). The limiting current density is the current density at which fuel is being consumed at the same rate it is being supplied to the triple-phase boundary. This parameter is affected by the thickness and diffusivity of the electrodes. Therefore, the required partial pressure of hydrogen at the triple-phase boundary is zero when operating at the limiting current density. Using the governing binary diffusion equation in terms of partial pressures, the binary diffusion equation is simplified to Eq. (7) after setting the partial pressure of hydrogen equal to zero at the triple-phase boundary:

$$i_{L(a)} = \frac{2FP^0_{H_2} D_{\mathrm{eff}(a)}}{R_u T d_a} \quad (7)$$

Assuming ideal gas behavior, kinetic theory with empirical data gives the following relationship for the effective diffusion coefficient $D_{\mathrm{eff}(a)}$.

$$D_{\mathrm{eff}(a)} = 1.37 \times 10^{-9} T^{-1.5} - 2.78 \times 10^{-5} \quad (8)$$

A similar set of equations governs cathode concentration polarization terms.

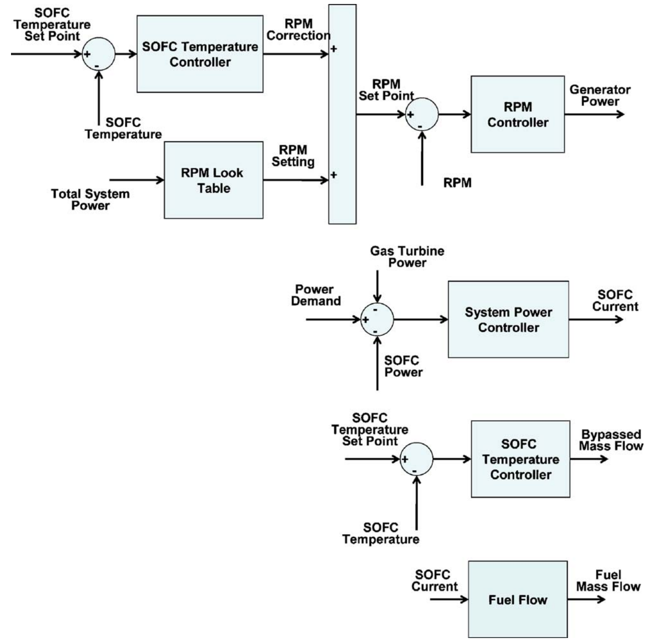

Fig. 3 Controller design

Approach

The work presented in this paper is on the controller design and dynamic analysis of a SOFC/GT hybrid system. Two different cases are presented: (1) a base-load system is exposed to changing ambient temperature and (2) a load-following system is exposed to the same ambient conditions while following a load demand curve.

The design electrical power production of the SOFC/GT hybrid system is 1.15 MW. For the base-load case, the system maintains 1.15 MW (1150 kW) of net electrical power production. The SOFC/GT hybrid system is operated in an extreme environment with a highly fluctuating ambient temperature. The ambient temperature is varied from $-5°C$ to $30°C$ in a sinusoidal form to emulate the daily temperature fluctuation. This range of temperatures accounts for colder regions and hot regions where the system may be operated.

The system is tested in load-following mode with a varying load demand. The varying load is of low frequency and is essentially seen a based load operation that is slowly adjusted throughout the day. The system is subjected to the same daily ambient conditions in all cases, while meeting a sinusoidal demand of power from 1150 kW at the peak of the day to 950 kW at the minimum power production of the day.

In this study, the controllers are not tuned for optimal performance; rather, this paper focuses upon the architecture of the controller design.

Controller Design. A decentralized controller design is used to control the hybrid system. The objective of the system controllers is to maintain constant power production while maintaining the SOFC operating temperature close to its design operation temperature of $900°C$. Figure 3 presents the controller design. The controller design consists of a gas turbine shaft speed controller, system power controller, SOFC average temperature and fuel flow controller. The shaft speed controller is a cascade controller with the outer loop consisting of a feed forward and a feedback controller for the RPM set point. The inner loop manipulates the gas turbine power to achieve the RPM set point provided by the outer loop. The feed forward aspect of the outer loop uses a look-up table to determine the RPM setting for a given system power. The feedback loop corrects the RPM setting for any SOFC average temperature deviations. The feedback portion is very important when the compressor is operating at an off design setting. For example, extreme ambient conditions would require RPM correction.

The system power controller manipulates the SOFC current in order to meet the power demand. The gas turbine power is treated as a disturbance for this particular controller. Therefore, the SOFC power is altered continuously by manipulating the current to meet the power demand that has not been met by the gas turbine.

There is additional control of the SOFC temperature via the bypass valve located between the turbine exhaust and the recuperator. The bypass, when used, lowers the inlet temperature to the SOFC module. The fuel flow is manipulated to achieve fuel utilization of 85%. The fuel flow controller is a feed forward controller based on the current of the SOFC. The fuel utilization after one pass through the anode section is approximately 53%.

The design electrical power production of the SOFC/GT hybrid system is 1.15 MW. For the base-load case the system maintains 1.15 MW (1150 kW) of net electrical power production. The SOFC/GT hybrid system is operated in an extreme environment with a vast fluctuating ambient temperature. The temperature changes account for colder or frigid regions and hot regions where the system may be operated.

The system is tested in load-following mode with a varying load demand. The same daily ambient conditions are applied to the system while demanding a sinusoidal power profile that varies from 1150 kW at the peak of the day to 950 kW at the minimum power production time of the day.

Results

Base-Load Case. The SOFC hybrid system is simulated in base-load mode. The system is to produce its design power while operating in varying ambient conditions. As stated before the ambient temperature is varied in the range of $\pm 20°C$. A sinusoidal temperature profile with a period of one day is used. The peak temperature is at 12 noon.

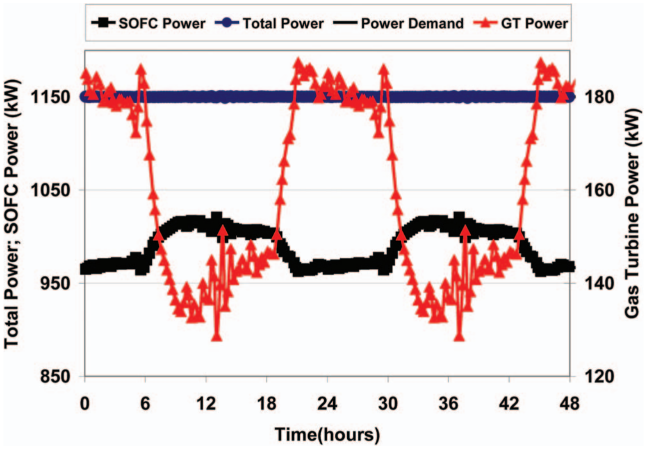

Fig. 4 Total power, SOFC power, and gas turbine power produced

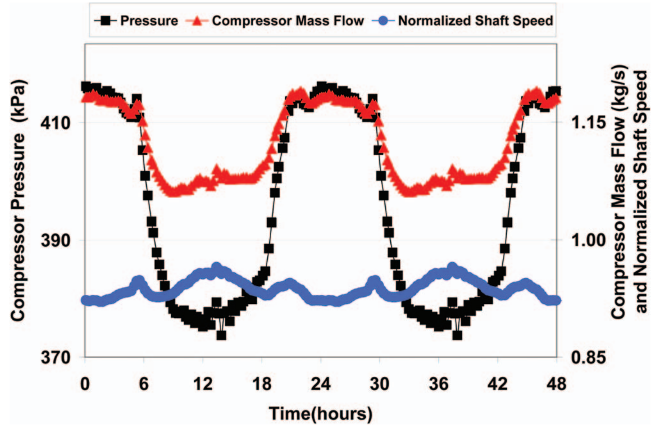

Fig. 6 Compressor mass flow, pressure, and normalized shaft speed

Figure 4 presents the total power produced by the hybrid plant along with the SOFC and the gas turbine power. The total power produced by the hybrid plant is constant with very small deviations. The gas turbine power changes dramatically to control the shaft speed. The SOFC power changes in order to compensate for the changes in the gas turbine power. Note that the simulations are computed using a much smaller time step than that presented by the symbols. Some details of the transient responses are lost so that a full two-day simulation can be presented. The simulation uses a variable time step solver with typical time step on the order of one second.

The SOFC average temperature is presented in Fig. 5 along with ambient temperature and percent bypass mass flow. The SOFC temperature is maintained within $\pm 20^\circ$C of the design operating temperature of 900°C. The effects of the ambient temperature are seen when plotted with the SOFC temperature. The high ambient temperature increases the compressor outlet temperature and also decreases the compressor mass flow by reducing the air density. The reduction of the compressor mass flow can be seen in Fig. 6. The dip in SOFC temperature just before 7 h is a result of the slight increase in mass flow from the compressor presented in Fig. 6 just before the mass flow sharply decreases. The mass flow from the compressor increases with the sudden increase of the shaft speed also presented in Fig. 6.

Two things promote this increase in shaft speed: (1) the ambient temperature is at the design inlet temperature of the compressor resulting in a more efficient compressor and (2) the TIT in Fig. 7 increases providing more power to the shaft. The gas turbine power increases in Fig. 1.

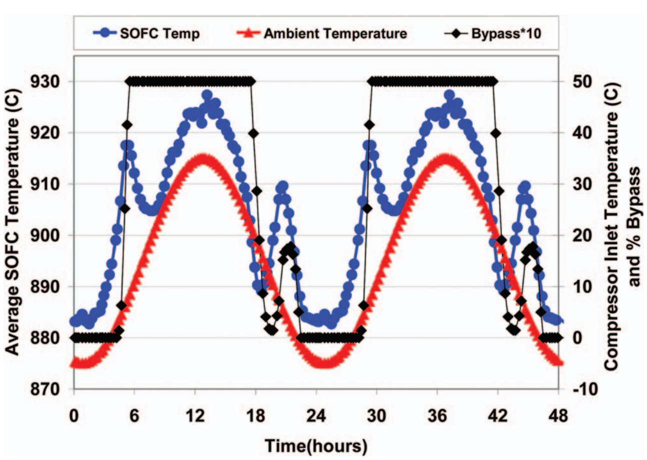

Fig. 5 SOFC average temperature, ambient temperature, and bypassed mass flow

It is shown in Fig. 4 that at 6 h it is possible to overcome this surge of net power being produced by the gas turbine. The TIT eventually lowers as the bypass valve opens and the ambient temperature continues to rise. This reduces the power produced by the turbine and thus increases the compressor work. The gas turbine power is dramatically decreased by the controllers at 7 h (Fig. 1).

According to Fig. 4, it is possible to allow the shaft speed to increase so that the SOFC can be provided sufficient air for cooling. Even though the gas turbine power is dramatically reduced, the shaft speed does not increase sufficiently. The extra work by the compressor prevents the shaft from speeding up and supplying more mass flow. The reduction of mass flow in the system reduces the operating pressure of the system in Fig. 6.

The bypass valve prevents the SOFC from overheating when the mass flow from the compressor does not fully recover. The bypass valve opens to reduce the temperature of the air entering the SOFC module. The effects of the bypass valve on the SOFC operating temperature are shown in Fig. 5. The SOFC inlet temperature (state #1 of Figs. 1 and 2) is reduced, as shown in Fig. 7. This decreases the cathode inlet temperature (see state #4 of Fig. 2), which helps prevent the SOFC stack from overheating. The cathode and turbine inlet temperature along with catalytic oxidizer temperature are presented in Fig. 7. The SOFC operating temperature rises at around 20–21 h. The bypass valve closed rapidly at this time, triggering this sudden rise in SOFC temperature. The bypass valve partially opens again when the SOFC temperature exceeds 900°C.

Figure 8 shows that the system efficiency fluctuates between 65% and 72%. At the peak ambient temperature, the gas turbine net power is reduced to sustain sufficient mass flow from the compressor. The SOFC power is increased to offset the power drop from the gas turbine. The increased power from the SOFC increases the fuel flow, which decreases the system efficiency when more fuel is required for the same net power produced by the system. The SOFC fuel utilization presented in Fig. 1.

Figure 8 also shows the fuel utilization after one pass through the anode section of the SOFC stack. After recirculation, the overall SOFC module electrochemical fuel utilization is 85%.

Load-Following Case. The same ambient temperature perturbation as presented in the previous case is applied to the hybrid system in the case presented in this section. In addition, the hybrid system must follow a load demand perturbation. The load demand

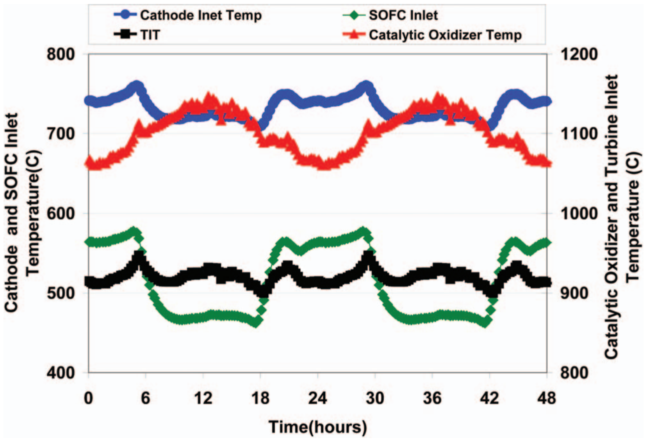

Fig. 7 SOFC, cathode, turbine inlet temperature, and the catalytic oxidizer temperature

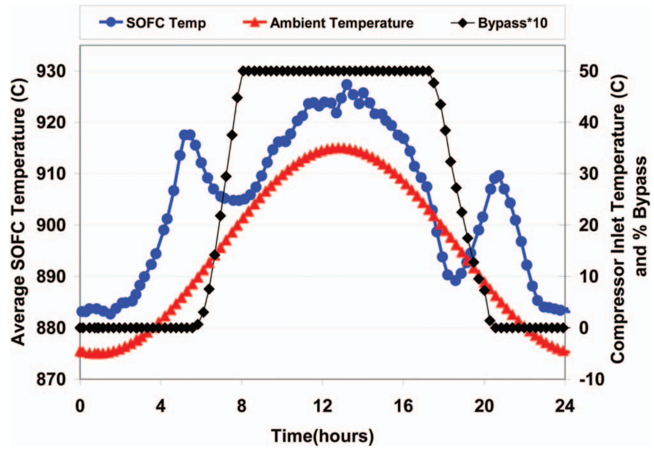

Fig. 10 SOFC average temperature, ambient temperature, and bypassed mass flow

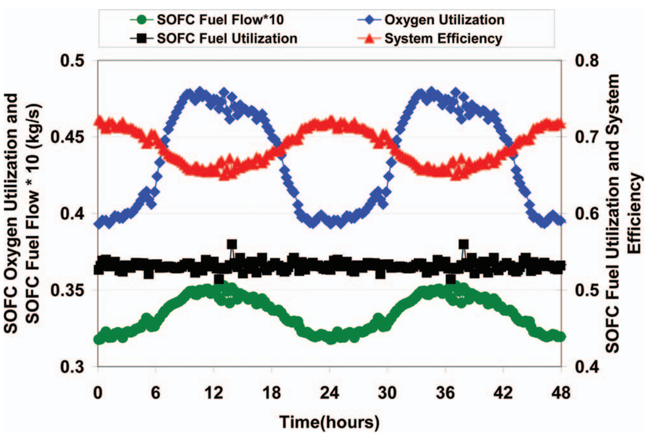

Fig. 8 System efficiency, SOFC oxygen and fuel utilization, and fuel flow

varies from 950 kW to 1150 kW. A sinusoidal power demand with a period of one day is used. The peak demand is at 12 noon.

The total power, SOFC power, and gas turbine power are presented in Fig. 9. The system was excellent in following the power demand variation. The fluctuations in gas turbine power can be

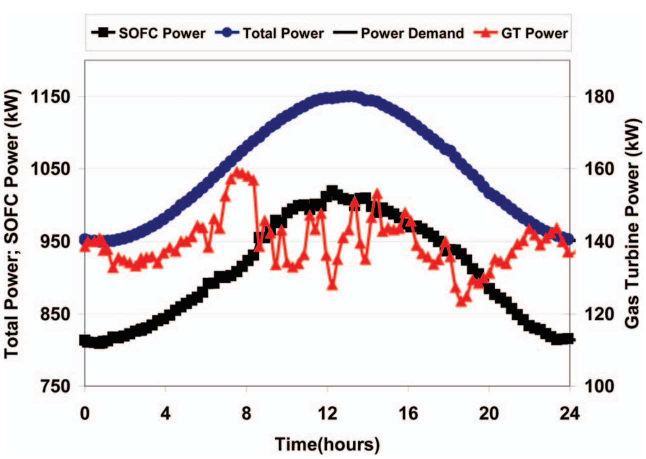

Fig. 9 Total power, SOFC power, and gas turbine power produced

seen in Fig. 9. The gas turbine remains around 140 kW during the entire day. Unlike the case before, the gas turbine does not reach 180 kW during the colder parts of the day since the system is operating at a lower power demand at that time of day. The SOFC power has a sinusoidal profile with fluctuations due only to the gas turbine power. If the ambient temperature had not been so extreme at 12 h, the gas turbine would have produced more net power.

The SOFC average temperature in Fig. 10 is kept within 25°C of the design temperature as in the case presented earlier. The impact of the ambient temperature on the system can be seen in Fig. 10. The same spikes and dips occur in the SOFC temperature as did in the previous case, but the logic behind them is more obvious in these results. The dip in SOFC temperature at 8 h is a result of the sudden increase in mass flow from the compressor presented in Fig. 11. The bulge in mass flow at 7 h is more apparent in this case (see Fig. 9). The mass flow from the compressor increases with the sudden increase of the shaft speed, also presented in Fig. 11. The same two causes as described in the previous section triggered this sudden change in shaft speed (1) more efficient compressor and (2) increase in TIT. The gas turbine power increases in Fig. 9 at the same time to overcome this surge of net power being produced by the gas turbine. The TIT eventually lowers as the bypass valve opens and the ambient temperature continues to rise. This reduces the power produced by the turbine and increases the compressor work as before. The gas turbine power is decreased by the controllers in Fig. 9 to allow the shaft speed to continually increase so that the SOFC can have sufficient cooling. In this case, the gas turbine power does not have to change as much since it is already at the right power range for 1150 kW system power production with 35°C ambient temperature.

Figure 12 presents the cathode and SOFC inlet temperature. The drop in both of these temperatures from the opening of the bypass valve can be seen between 7 and 17 h. There is a more dramatic change in the SOFC inlet than the cathode inlet temperature because the heat exchanger becomes more effective due to the increase in temperature differences between the SOFC inlet and catalytic oxidizer temperature. The catalytic oxidizer temperature increases from the increase in SOFC power (more anode off-gas), SOFC temperature, and the reduction of oxidant mass flow (higher oxygen utilization, Fig. 13). The TIT increases because of the catalytic oxidizer temperature increase, but less since the heat exchanger is more effective in transferring the heat from one flow than from the other.

The system efficiency in Fig. 13 has the same profile as in the earlier case, but is higher when the power production is lower due to the higher operating voltage or more efficient operation of the

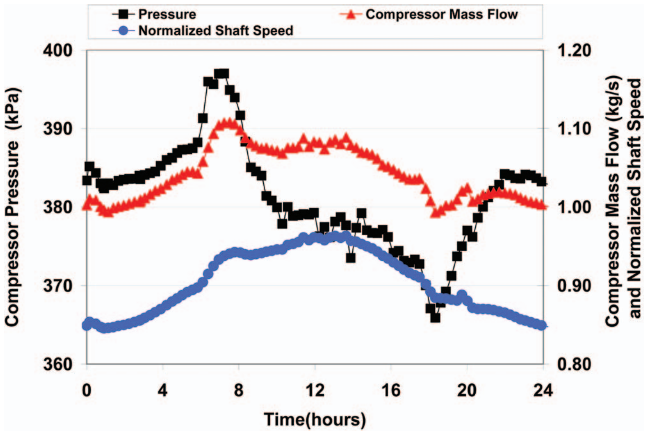

Fig. 11 Compressor mass flow, pressure, and normalized shaft speed

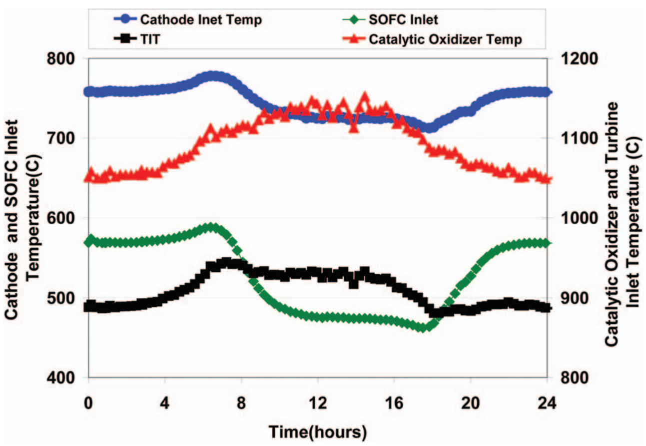

Fig. 12 SOFC, cathode, turbine inlet temperature, and the catalytic oxidizer temperature

SOFC. The oxygen utilization and the fuel utilization are similar to the case presented in the previous section. The oxygen utilization does reach higher levels of 47%, which indicates that the mass flow would be desired to be increased for better performance.

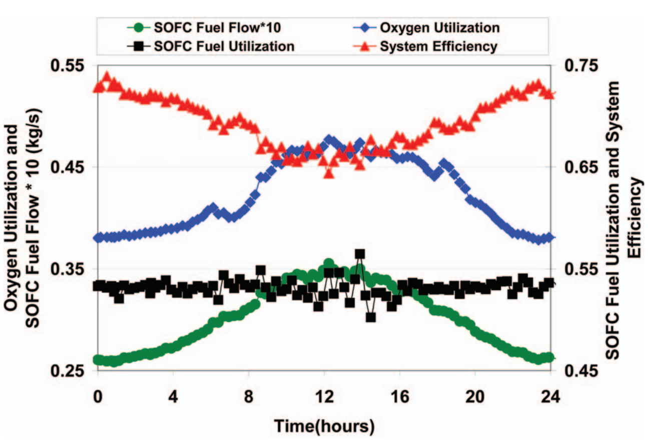

Fig. 13 System efficiency, SOFC oxygen and fuel utilization, and fuel flow

Summary and Conclusions

A SOFC/GT hybrid system was developed with controllers that allow load-following capabilities. A base-load case with varying ambient temperature for two days was simulated and presented. The system maintains constant power (100% design power) while being exposed to an ambient temperature that varies significantly from -5°C to $+35^\circ$C. The system controllers responded to changes in the ambient temperature and successfully maintained the SOFC operating temperature within 20°C of the design operating temperature. The gas turbine power had to be continuously manipulated in order maintain the correct shaft speed and in turn the adequate amount of compressor mass flow.

A sinusoidal load profile was demanded of the hybrid system with peak power demand at 12 h at the same time of the peak ambient temperature. The system followed the load very well. In this case, the gas turbine remained closer to 140 kW during the entire load perturbation. The oxygen utilization increased during the load perturbation.

Ideally for a SOFC/GT hybrid system, much like a gas turbine system, the oxygen and fuel utilization would remain constant over the entire range of load demand. This fixes the air-to-fuel ratio in the SOFC module. A controller that enforces constant oxygen utilization is needed to maintain consistent SOFC average temperature and operation. Precisely controlling the compressor mass flow during large fluctuations in ambient temperature is challenging. If not carefully executed, the gas turbine can become unstable. The constant RPM approach with temperature error correction attempts to control the mass flow, but there are deviations in the SOFC temperature and oxygen utilization. These deviations are acceptable and the RPM control of the gas turbine provides a more stable means of controlling the system.

In future work, a combination of RPM control and direct mass flow control will be investigated. This type of control approach will provide stability and accurate control of the system mass flow.

Nomenclature

d = thickness of electrode, m
D_{eff} = effective diffusion coefficient, kmol/m^2
E_0 = standard theoretical potential, V
F = Faraday's constant, coulombs/mol electron
FC/GT = fuel cell/gas turbine hybrid
GT = gas turbine
i = current density of the node, A/m^2
i_0 = exchange current density, A/m^2
$i_{L(a)}$ = limiting current density for anode electrode, A/m^2
MCFC = molten carbonate fuel cell
MCFC/GT = molten carbonate fuel cell/gas turbine hybrid
n = number of contributing electrons $n=2$
NETL = National Energy Technology Laboratory
NFCRC = National Fuel Cell Research Center
P = partial pressure of species i in the bulk flow, Pa
R_{eff} = ohmic polarization loss, ohm m^2
R_u = ideal gas constant, kJ/(K* kmol)
SOFC = solid oxide fuel cell
SPC = Siemens Power Corporation
SPC-SOFC = Siemens Power Corporation solid oxide fuel cell
TIT = turbine inlet temperature
T = temperature of reaction, K
α = dimensionless transfer coefficient
η_A = activation polarization loss, V
η_C = concentration polarization loss, V
η_R = ohmic polarization loss, V

References

[1] Bessette, N. F., 1994, "Modeling and Simulation for SOFC Power Systems," *Mechanical Engineering*, Georgia Institute of Technology, Atlanta, p. 209.

[2] Costamagna, P., Magistri, L., and Massardo, A. F., 2001, "Design and Part-Load Performance of a Hybrid System Based on a Solid Oxide Fuel Cell Reactor and a Micro Gas Turbine," J. Power Sources, **96**(2), pp. 352–368.

[3] Costamagna, P., Selimovic, A., Del Borghi, M., and Agnew, G., 2004, "Electrochemical Model of the Integrated Planar Solid Oxide Fuel Cell (IP-SOFC)," Chem. Eng. J., **102**(1), pp. 61–69.

[4] Massardo, A. F., and Lubelli, F., 2000, "Internal Reforming Solid Oxide Fuel Cell-Gas Turbine Combined Cycles (IRSOFC-GT): Part A—Cell Model and Cycle Thermodynamic Analysis," ASME J. Eng. Gas Turbines Power, **122**, pp. 27–35.

[5] Rao, A. D., and Samuelsen, G. S., 2002, "Analysis Strategies for Tubular Solid Oxide Fuel Cell Based Hybrid," ASME J. Eng. Gas Turbines Power, **124**, pp. 503–509.

[6] Yi, Y., Smith, T. P., Brouwer, J., and Rao, A. D., 2003, "Simulation of a 220 kW Hybrid SOFC Gas Turbine System and Data Comparison," Proc.-Electrochem. Soc., **7**, pp. 1442–1454.

[7] Gemmen, R. S., Liese, E., Rivera, J. G., Jabbari, F., and Brouwer, J., 2000, "Development of Dynamic Modeling Tools for Solid Oxide and Molten Carbonate Hybrid Fuel Cell Gas Turbine Systems," ASME Paper No. 2000-GT-0552.

[8] Liese, E. A., Gemmen, R. S., Jabbari, F., and Brouwer, J., 1999, "Technical Development Issues and Dynamic Modeling of Gas Turbine and Fuel Cell Hybrid Systems,"ASME Paper No. 99-GT-360.

[9] Liese, E. A., and Gemmen, R. S., 2002, "Dynamic Modeling Results of a 1 MW Molten Carbonate Fuel Cell/Gas Turbine Power System," ASME Paper No. GT-2002-30110.

[10] Lukas, M. D., Lee, K. Y., and Ghezel-Ayagh, H., 1999, "Development of a Stack Simulation Model for Control Study on Direct Reforming Molten Carbonate Fuel Cell power Plant," IEEE Trans. Energy Convers., **14**, pp. 1651–1657.

[11] Lukas, M. D., Lee, K. Y., and Ghezel-Ayagh, H., 2000, "Operation and Control of Direct Reforming Fuel Cell Power Plant," IEEE Trans. Energy Convers., **14**, pp. 1651–1657.

[12] Lukas, M. D., Lee, K. Y., and Ghezel-Ayagh, H., 2002, "Modeling and cycling control of carbonate fuel cell power plants," Control Eng. Pract., **10**(2), pp. 197–206.

[13] Rivera, J. G., 2000, "Numerical Analysis of a Molten Carbonate Fuel Cell," Master's thesis, University of California, Irvine, Irvine, CA.

[14] Roberts, R. A., 2005, "A Dynamic Fuel Cell-Gas Turbine Hybrid Simulation Methodology to Establish Control Strategies and an Improved Balance of Plant," Ph.D. thesis, University of California, Irvine, Irvine, CA, p. 316.

[15] Roberts, R. A., and Brouwer, J., 2006, "Dynamic Simulation of a Pressurized 220 kW Solid Oxide Fuel Cell-Gas Turbine Hybrid System: Modeled Performance Compared to Measured Results," ASME J. Fuel Cell Sci. Technol., **3**, pp. 18–25.

[16] Roberts, R. A., Mason, J., Jabbari, F., Brouwer, J., Samuelsen, S., Liese, E., and Gemmen, R., 2003, "Inter-Laboratory Dynamic Modeling of a Carbonate Fuel Cell for Hybrid Application," ASME Paper No. GT2003-38774.

[17] Roberts, R. A., Brouwer, J., Liese, E., and Gemmen, R. S., 2004, "Dynamic Simulation of Carbonate Fuel Cell-Gas Turbine Hybrid Systems," ASME Paper No. GT2004-53653.

[18] Roberts, R. A., Brouwer, J., Liese, E., and Gemmen, R. S., 2005, "Development of Controls for Dynamic Operation of Carbonate Fuel Cell-Gas Turbine Hybrid Systems," ASME Paper No. GT2005-68774.

[19] Willis, J., 2005, "Capstone Microturbines," *ICEPAG*, Sep. 7–8, 2005, APEP, Irvine, CA.

[20] Kim, J.-W. et al., 1999, "Polarization Effects in Intermediate Temperature, Anode-Supported Solid Oxide Fuel Cells," J. Electrochem. Soc., **146**(1), pp. 69–78.

[21] Magistri, L., Traverso, A., Cerutti, F., Bozzolo, M., Costamagna, P., and Massardo, A. F., 2005, "Modeling of Pressurized Hybrid Systems Based on Integrated Planar Solid Oxide Fuel Cells (IP-SOFC) Technology," Fuel Cells, Topical Issue "Modelling of Fuel Cell Systems," **1**(5), Wiley-VCH.